EXPERIMENTAL STUDIES OF ADVECTION-REACTION-DIFFUSION SYSTEMS*

T. H. SOLOMON†, M. S. PAOLETTI‡ AND M. E. SCHWARTZ§

Department of Physics and Astronomy, Bucknell University
Lewisburg, PA 17837, U.S.A.

We present the results of experiments on the effects of chaotic fluid mixing on the dynamics of reacting systems. The flow studied is a chain of alternating vortices in an annular geometry with drifting and/or oscillatory time-dependence. The dynamical system is the oscillatory or excitable state of the well-known Belousov-Zhabotinsky chemical reaction. Results from two sets of experiments are as follows: (1) Fronts propagating in the oscillating vortex chain are found to mode-lock onto the frequency of the external oscillations. It is also found that the presence of a significant "wind" (drift of the vortices in the lab frame) causes fronts propagating against the wind to freeze. (2) Synchronization of oscillating reactions in an extended flow (vortex chain with large number of vortices) is found to be enhanced significantly by the presence of superdiffusive transport characterized by Lévy flights that connect different parts of the flow.

1. Introduction

There has been a significant amount of research during the past three decades on front propagation and pattern formation in *reaction-diffusion* (RD) systems[1,2]. The paradigm for RD systems is the Belousov-Zhabotinsky (BZ) chemical reaction[3,4], a reaction that can oscillate almost periodically for several hours when well-mixed. When poured into a petri dish with no flow, however, target and spiral patterns form, due to an interaction between local oscillations of the chemistry and diffusive coupling between different parts of the system. The BZ system has been studied extensively since the patterns formed are similar in many respects to those found in a wide variety of RD systems, including spiral waves of electrical activity in the heart[5], waves of "spreading depression" in the

* This work is supported by US National Science Foundation grants DMR-0404961, DMR-0703635 and PHY-055290.

† Email address: tsolomon@bucknell.edu.

‡ Current address: Department of Physics, University of Maryland, College Park, MD 20742, USA; email: paoletti@umd.edu.

§ Current address: Department of Physics, Columbia University, New York, NY 10027, USA; email: mes2140@columbia.edu.

brain that are responsible for migraine headaches[6], and patterns that form in populations of slime mold in a dish[7].

By definition, an RD system has no fluid flows. Most fluid systems, however, are not stagnant; fluid flows dramatically enhance mixing well beyond that due to molecular diffusion alone. Despite the importance of fluid mixing on the pattern formation process, the more general *advection-reaction-diffusion* (ARD) problem has only recently begun to receive significant attention, and most of this attention has been theoretical[8,9,10,11,12,13,14]. The issue is of particular interest in light of studies[15] that indicate that fluid mixing can be *chaotic* even for simple, well-ordered, laminar fluid flows. The importance of chaotic mixing in ARD systems has particular relevance for the design of microfluidic devices ("factories-on-a-chip"), cellular-scale processes in biological systems and for understanding the spreading of diseases in a moving population.

In this article, we present results of some experimental studies of ARD dynamics. The reaction is the Belousov-Zhabotinsky reaction, and the flow is a chain of counter-rotating vortices with both oscillatory and drifting time-dependence, a flow that has been shown to produce chaotic mixing. Two experiments are discussed: (1) the effects of cellular flows on the propagation of fronts; and (2) the effects of chaotic mixing and superdiffusive transport on the collective dynamics and synchronization of oscillatory reactions.

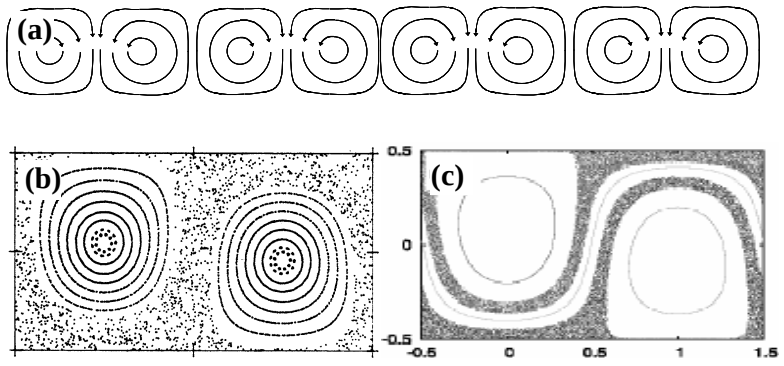

Figure 1. (a) Sketch of the alternating vortex chain. The entire chain of vortices can oscillate and/or drift in the lateral direction. (b) Poincaré section for oscillating vortex chain, showing ordered regions of transport in vortex cores and chaotic region around and between vortices. (c) Poincaré section for oscillating and drifting vortex chain.

The alternating vortex chain flow and its mixing properties are discussed in Section 2. Details about how the flow is produced experimentally and about the chemistry are presented in Section 3. In Section 4, we describe the experiments on front propagation in this system, along with numerical simulations of the same phenomena. Experiments on the collective dynamics of oscillating reactions – and the impact of chaotic mixing on these dynamics – are described in Section 5.

2. Chaotic mixing in the alternating vortex chain.

The alternating vortex chain used in these studies is shown schematically in Figure 1. A simple model of the velocity field of this flow (assuming free-slip boundary conditions and no three-dimensional components to the flow) is as follows:

$$\begin{aligned} \dot{x} &= -U\frac{\lambda}{2d}\cos(\frac{2\pi}{\lambda}x_s)\sin(\frac{\pi y}{d}) \\ \dot{y} &= U\sin(\frac{2\pi}{\lambda}x_s)\cos(\frac{\pi y}{d}) \\ x_s &= x + \frac{v_0}{\omega}\sin\omega t + v_d t \end{aligned} \tag{1}$$

The vortex chain can oscillate and/or drift in the lateral direction with maximum oscillation speed v_o and drift speed v_d.

If the flow is stationary ($v_o = v_d = 0$), then tracers in the flow follow closed, ordered trajectories within the vortices. Long-range transport is achieved via a combination of advection of tracers around the vortices and diffusion of tracers across the separatrices between vortices[16,17]. If the vortex chain oscillates laterally ($v_o \neq 0$, $v_d = 0$), tracers near the separatrices follow chaotic trajectories[18,19] and move between adjacent vortices, as shown in a Poincaré section (Figure 2a). Tracers near the vortex centers follow ordered trajectories, remaining confined to a single vortex. Long-range transport in this flow has been shown experimentally to be typically enhanced diffusion, with a variance $\sigma^2(t) = 2D^*t$ with D^* an enhanced diffusion coefficient.

The addition of drift to the vortex chain ($v_o \neq 0$, $v_d \neq 0$) changes the chaotic mixing. If $v_d > v_o$, the chaotic region often divides into two separate regions, with an additional ordered, snake-like region winding around and between the vortices. Transport in this case is superdiffusive with the variance growing as

$\sigma^2(t) \sim t^\gamma$ with $1 < \gamma < 2$. Tracers in a chaotic region in this case follow *Lévy flight* trajectories, alternately sticking to ordered regions within vortex cores and undergoing long, snake-like flights between distant parts of the vortex chain. The oscillating/drifting vortex chain is notable by the fact that superdiffusion can be "turned on" or "turned off" by adjusting the relative magnitudes of v_o and v_d.

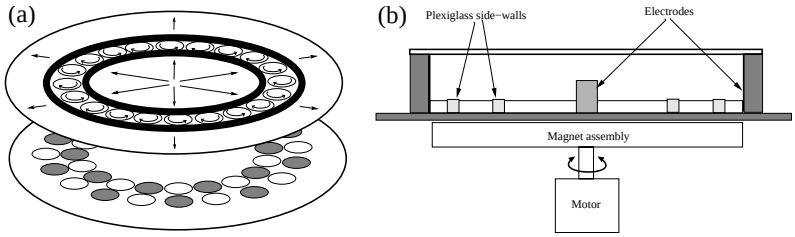

Figure 2. Experimental apparatus. (a) Exploded view of magnetohydrodynamic forcing, along with the annular vortex chain. (b) Side view of apparatus.

3. Experimental methods

The flow is generated with a magnetohydrodynamic technique, shown in Figure 2. Two rings of ¾"-diameter magnets are arranged in a circular piece of plexiglass, which is mounted coaxially onto a voltage-programmed motor. Above this magnet assembly is a shallow cylindrical container with a central electrode, an outer electrode, and two (slightly raised) plastic rings which define the region of interest. A thin layer (2 mm deep) of an electrolytic solution (usually the BZ chemicals) carries a radial electrical current that interacts with the magnets to produce an annular chain of vortices. Lateral movement of the vortex chain is accomplished by rotating the magnet assembly either periodically (for oscillating time dependence), with a constant angular velocity (for drifting time dependence) or a combination of the two.

Previous publications describe the chemistry used for the excitable[20,21] and oscillatory[22,23] BZ reaction in these experiments. A key aspect of the excitable reaction is the use of Ruthenium as a catalyzer. The Ru-catalyzed BZ reaction is photosensitive; illumination with blue/green light inhibits the reaction. We use a video projector to project a red ring over most of the annular region, and blue/green everywhere else to limit the reaction to the region of interest and to

control its propagation direction. Details about the techniques are described in Ref. 21.

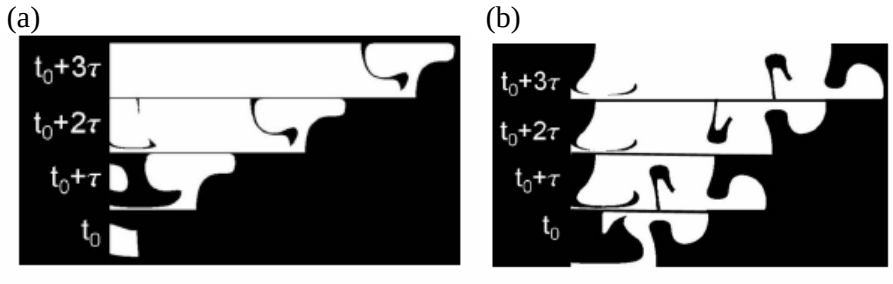

Figure 3. Simulations showing mode-locking with (N,M) = (1,1) for (a) and (1,2) for (b).

4. Front propagation

4.1. *Mode-locking in oscillating vortex chain*

A numerical study of front propagation by Cencini et al[10] predicted mode-locking of fronts in the oscillating vortex chain. In general, mode-locking is when an oscillating system matches its frequency to that of a periodic external driving. In the case of a front propagating in the oscillating vortex chain, mode-locking is manifested as the front moving an integer number N of wavelengths (with one wavelength equal to two vortices in the flow) in an integer number M of drive periods. Simulations of mode-locking are shown in Figure 3; experimental sequences of similar mode-locking behavior are shown in Figure. 4.

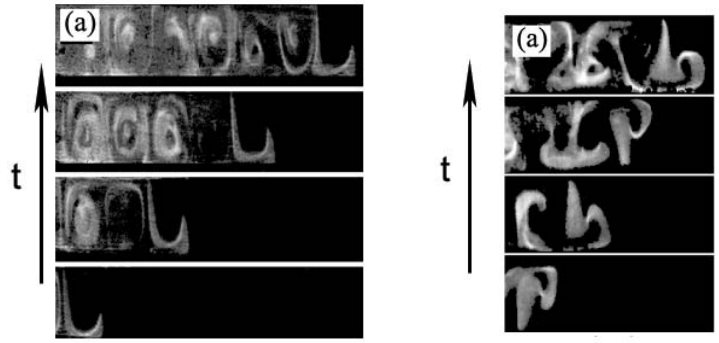

Figure 4. Experimental sequences showing mode-locking with (N,M) = (1,1) for (a) and (1,2) for (b). Each image is acquired one period of oscillation after the previous one.

The velocity at which a mode-locked front propagates is well defined: $v_f = N\lambda/MT = (N/M)\lambda f$. Velocities of propagating fronts are plotted in Figure 5a, along with the theoretical predictions for mode-locked velocities. (There are no fitted parameters in these plots.) Mode-locking is apparent over a wide range

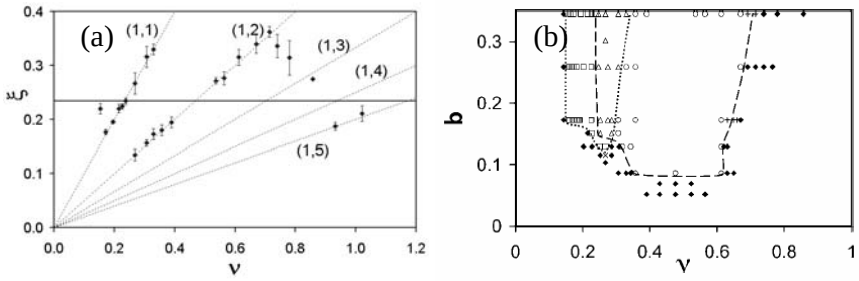

Figure 5. (a) Experimental results showing non-dimensional front speed ξ as a function of non-dimensional frequency ν. The dotted lines show the theoretical predictions (with no fitted parameters) for mode-locked speeds. (b) Parameter-space plot showing Arnol'd tongues for (1,1) and (1,2) mode-locked states. Filled diamonds denote unlocked states, whereas open squares, open circles and open triangles denote states with (1,1), (1,2) and combination (1,1)/(1,2) mode-locking, respectively.

of frequencies for both the (1,1) and (1,2) mode-locking regimes. There is also a significant region of overlap between the two where the velocity alternately (and erratically) switches between the (1,1) and the (1,2) mode-locking values. A parameter-space diagram showing the amplitudes and frequencies for the (1,1) and (1,2) mode-locking regimes is shown in Figure 5b. Once again, a significant overlap region is found.

Mode-locking behavior is quite robust in this system. It is of interest that the numerical predictions are for a two-dimensional flow with free-slip boundary conditions, whereas the experimental flow has no-slip boundary conditions and a weak, secondary, three-dimensional flow due to Ekman pumping[24]. Despite these quite significant differences in the details of the flow, the mode-locking behavior seen in the experiments is identical to that predicted numerically.

4.2. *Freezing of fronts in the presence of a uniform wind*

The drifting vortex chain ($v_o = 0$, $v_d \neq 0$) is mathematically equivalent – if a transformation is made to a co-drifting reference frame – to a stationary vortex chain with an imposed uniform wind. For a front propagating against this wind (in the co-drifting frame), three types of behavior are possible[25]: (1) if the wind

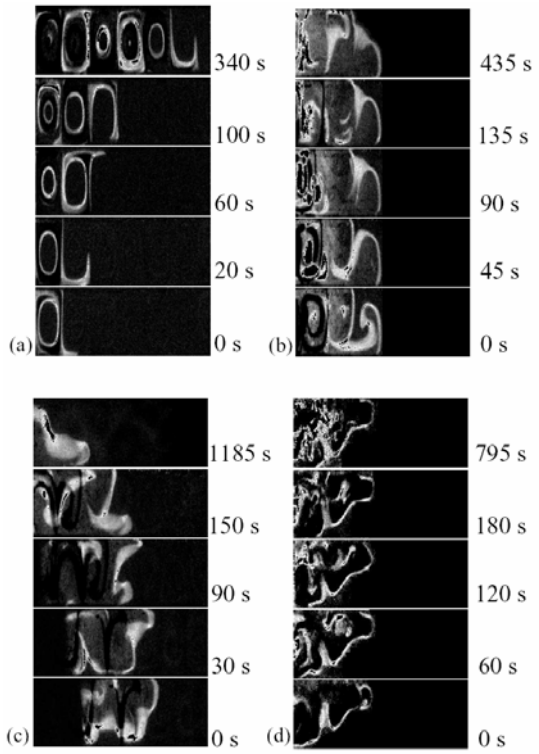

Figure 6. Experimental sequences showing front propagation in the presence of an opposing, uniform wind blowing right-to-left. (a) Small wind; front propagates forward to the right. (b) Intermediate wind; front is frozen in the leading vortex. (c) Strong wind; front is blown back to the left by the wind. (d) Sequence showing front frozen in a random vortex flow with opposing wind.

(denoted non-dimensionally as $\varepsilon = W/v_{rd}$, where v_{rd} is the reaction-diffusion – no flow – front propagation speed) is small, then the front propagates forward against the wind; (2) for intermediate values of ε, the front remains "frozen" – trapped in the leading vortex, neither propagating forward nor being blown back by the wind; (3) for large values of ε, the wind blows the front backwards. These three different regimes are shown in Figures 6a, b and c, respectively.

Figure 7 shows front velocities (denoted non-dimensionally by $\nu = v_f/v_{rd}$) for three different values of the non-dimensional vortex strength $\mu = U/v_{rd}$. The dashed diagonal line corresponds to the case with no vortex flow ($\mu = 0$); in this case, the effects of the wind are a simple Galilean transformation and $\nu = 1 - \varepsilon$. A striking feature of this behavior is the large range of wind speeds over which the fronts are frozen (ν = 0); for μ = 40, fronts remain frozen at almost 10 times the RD front propagation velocity. The width of the frozen front regime collapses onto the μ = 0 result for small vortex strength. The minimum wind for

freezing of fronts is ε = 1 for all values of μ. This makes sense, since a front

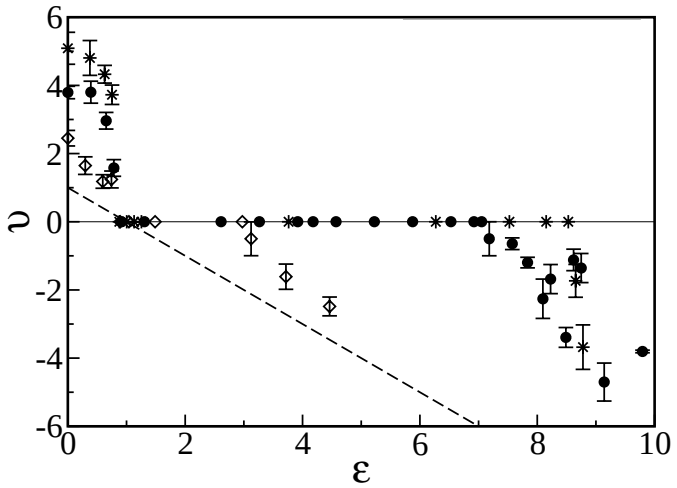

Figure 7. Non-dimensional front propagation speed ν as a function of non-dimensional wind ε with μ = 4 (open diamonds), 12 (filled circles) and 40 (asterisks). The dashed line is the theoretical limit for μ = 0.

must burn across a vertical separatrix between vortices to propagate forward. Since the flow is perpendicular to the front propagation direction at the separatrix, it can't propagate forward if the wind exceeds the RD propagation speed.

Freezing of reaction fronts is not limited to ordered vortex flows. Experiments have also been done with random vortex flows in which similar freezing behavior is seen (Figure 6d). Details of the experiments with random flows are reported elsewhere[25].

The experiments reported in this section are all with stationary flows. Nevertheless, the results should have implications for front propagation in a wide range of time-dependent, two-dimensional flows that are dominated by vortex behavior (which is very common in 2D flows). A moving vortex in a time-dependent flow can often be viewed (temporarily) in a co-moving reference frame as a stationary vortex with an imposed wind. From this perspective, a vortex passing through a reaction front traveling in the same direction should be expected to pin and drag the front.

Both the freezing front behavior in this section and the mode-locking behavior from the previous section indicate the critical importance of vortex

structures in the propagation of reaction fronts in a flow system. These experiments indicate the importance of considering coherent vortex structures in any general theory of front propagation in ARD systems.

5. Collective oscillatory behavior and synchronization by chaotic mixing

The ARD behavior is quite different if the oscillatory version of the BZ reaction is used in the vortex chain flow. In this case, each vortex and its contents act like an oscillating node of a network, and communication between these nodes is via chaotic mixing[23]. The problem is particularly interesting in light of recent studies of networks and the manner in which they are connected. As discussed in Section 1, oscillatory time-dependence of the vortex chain (or combination oscillation and drift with $v_d < v_o$) results in chaotic mixing with enhanced diffusive transport. Diffusive behavior is analogous to a network with well-ordered, nearest-neighbor connections. Superdiffusive transport (for $v_d > v_o$) is associated with Lévy flights that can travel long distances in a short period of time. These flights are similar in many respects to "short-cut" connections in *Small-World* network models[26]. So, the oscillating/drifting vortex chain flow gives us the ability to study how the large-scale collective behavior of a fluid-based network is affected by the type of transport (diffusive or superdiffusive).

If the vortices are stationary ($v_d = v_o = 0$), then communication between them is via molecular diffusion across the separatrices; coupling in this case is very weak and the vortices are essentially isolated. With the oscillatory BZ reaction in this flow, the contents of each vortex oscillate almost periodically, independent of the rest. Oscillations of the BZ reaction may start off initially synchronized (due to mixing in the apparatus when the chemicals are added) but de-synchronize within a few periods of the chemical oscillations. Ultimately, the chemicals in each vortex oscillate independently of the rest.

If oscillatory and/or drifting time-dependence is added to the vortex chain, three types of collective behavior are observed (Figure 8). In every situation in which the transport is diffusive (e.g, for $v_d < v_o$), aperiodic traveling waves are found, regardless of the initial conditions. (Figure 8a). Sometimes the waves travel counterclockwise around the annulus and sometimes clockwise. Often the waves emanate from a source and travel in both directions around the annulus to a sink on the other side, with the locations of the source and sink drifting with respect to the chain. The behavior sloshes continuously and unpredictable between these different states; we have not encountered a situation where the traveling waves remain consistent in their behavior.

If the transport is superdiffusive ($v_d > v_o$) then one of two types of global synchronization are observed. In most cases, "co-rotating" synchronization is osbsered (Figure 8b), where odd vortices are all synchronized with each and even vortices are all synchronized with each other, but where the phase difference between the two chains can be anything. The lack of synchronization between the two chains in this case is due to the isolation of the two chaotic regions that is usually (but not always) found for flows with $v_d > v_o$ (see Fig. 1c). Mixing in these chaotic regions skips adjacent vortices, connecting odd vortices to odd vortices and even vortices to even vortices. In some cases if v_d is just slightly larger than v_o, Lévy flight trajectories and superdiffusion are possible even for a situation with only one, connected chaotic region. In this case, global synchronization is found with the BZ chemicals in all vortices oscillating in unison (Figure 8c). More details about the experimental results are presented in Ref. 23.

The implication of these results is that superdiffusive transport may be a necessary (although probably not sufficient) condition for synchronization in an extended fluid system, i.e., one in which the total system size is appreciably larger than characteristic length scales of the fluid flow. These results could be important in interpreting synchronization behavior found in natural systems, such as algae blooms in the Gulf of Mexico and phytoplankton blooms in the Atlantic Ocean.

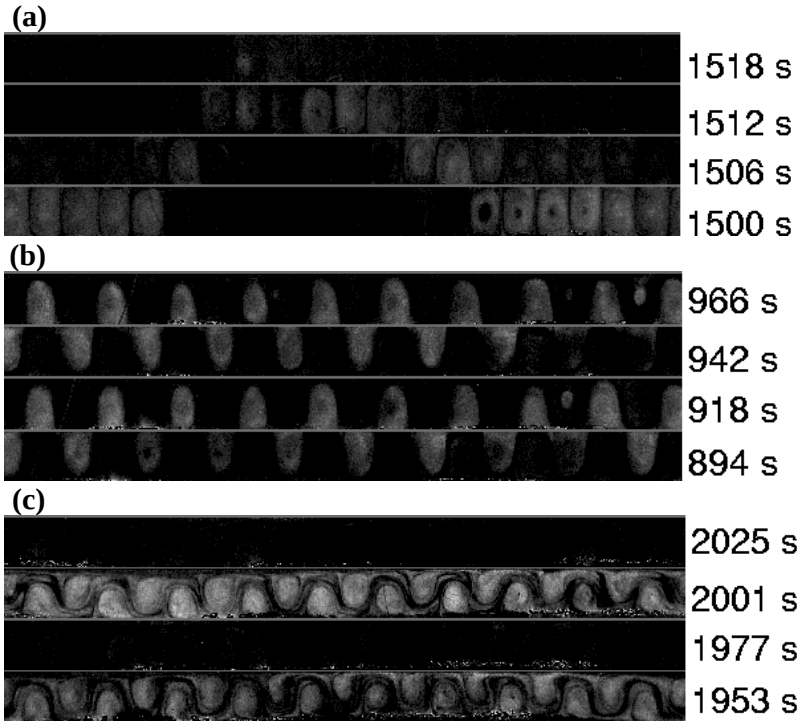

Figure 8. Sequences of images of BZ reaction in oscillating/drifting vortex chain. (a) Wave behavior seen when $v_d < v_o$. (b) Co-rotating and (c) global synchronization for $v_d > v_o$.

Acknowledgments

This work was supported by the US National Science Foundation Grants DMR-0404961, DMR-0703635, REU-0097424, and REU-0552790.

References

1 . P. Grindrod, *The Theory and Applications of Reaction-Diffusion Equations: Patterns and Waves* (Clarendon Press, Oxford, 1996).
2. D. Ben-Avraham & S. Havlin, *Diffusion and Reactions in Fractals and Disordered Systems* (Cambridge University Press, Cambridge, 2000).
3. A. T. Winfree, *Science* **175**, 634-636 (1972).
4. K. Showalter, *J. Chem. Phys.* **73**, 3735-3742 (1980).
5. Z. L. Qu, J. N. Weiss & A. Garfinkel, *A. J. Physiol. – Heart Circ. Physiol.* **276**, H269 (1999).
6. M. A. Dahlem & S. C. Muller, *Annalen der Physik* **13**, 442 (2004).

7. D. A. Kessler & H. Levine, *Phys. Rev. E* **48**, 4801 (1993).
8. T. Tel, A. de Moura, C. Grebogi & G. Karolyi, *Phys. Rep.* **413**, 91-196 (2005).
9. M. Abel, A. Celani, D. Vergni & A. Vulpiani, *Phys. Rev. E* **64**, 046307 (2001).
10. M. Cencini, A. Torcini, D. Vergni & A. Vulpiani, *Phys. Fluids* **15**, 679-688 (2003).
11. G. Karolyi, A. Pentek, Z. Toroczkai, T. Tel & C. Grebogi, *Phys. Rev. E* **59**, 5468-5481 (1999).
12. G. Karolyi, A. Pentek, I. Scheuring, T. Tel & Z. Toroczkai, *Proc. Nat. Acad. Sci. U.S.A.* **97**, 13661-13665 (2000).
13. A. Neufeld, *Phys. Rev. Lett.* **87**, 108301 (2001).
14. Z. Neufeld, I. Z. Kiss, C. Zhou & J. Kurths, *Phys. Rev. Lett.* **91**, 084101 (2003).
15. H. Aref, *J. Fluid Mech.* **143**, 1-21 (1984).
16. B. Shraiman, *Phys. Rev.A* **36**, 261 (1987).
17. T. H. Solomon & J. P. Gollub, *Phys. Fluids* **31**, 1372 (1988).
18. T. H. Solomon & J. P. Gollub, *Phys. Rev. A* **38**, 6280-6286 (1998).
19. T. H. Solomon, S. Tomas & J. L. Warner, *Phys. Rev. Lett.* **77**, 2682-2685 (1996).
20. M. S. Paoletti & T. H. Solomon, *Europhys. Lett.* **69**, 819-825 (2005).
21. M. S. Paoletti & T. H. Solomon, *Phys. Rev. E* **72**, 046204 (2005).
22. C. R. Nugent, W. M. Quarles & T. H. Solomon, *Phys. Rev. Lett.* **93**, 218301 (2004).
23. M. S. Paoletti, C. R. Nugent & T. H. Solomon, *Phys. Rev. Lett.* **96**, 124101 (2006).
24. T. H. Solomon and I. Mezic, *Nature* **425**, 376 (2003).
25. M. E. Schwartz and T. H. Solomon, *Phys. Rev. Lett.* (in press).
26. D. J. Watts & S. H. Strogatz, *Nature* **393**, 440 (1999).